

Modulating “Jousting” C–F---H–C Interactions with a Bit of Hydrogen Bonding

Mark D. Struble, Jessica Strull, Kishan Patel, Maxime A. Siegler, and Thomas Lectka*

Department of Chemistry, New Chemistry Building, Johns Hopkins University, 3400 North Charles Street, Baltimore, Maryland 21218, United States

S Supporting Information



ABSTRACT: We have synthesized a series of molecules wherein very close C–F---H–C σ -bond interactions, which we have termed “jousting”, can be perturbed through both *red*- and *blue*-shifted hydrogen bonding effects. These interactions were induced by the placement of various functional groups geminal to the H–C bond. “Jousting” interactions appear to be an admixture of F---H hydrogen bonding and C–H bond compression. The associated electronic effects from changes in the functional group at the X-position were also studied.

Over the last few decades, there has been a marked increase in the use of fluorine in chemistry, whether it be for medical/biological applications,¹ materials development,² or synthetic methodology.^{3,4} In particular, an estimated 20% of the current pharmaceuticals on the market contain fluorine, and there is a large amount of ongoing research investigating the effects of fluorination on the properties of natural products for drug discovery.^{5,6} In a recent review, fluorine was called the “second-favorite heteroatom” after nitrogen for drug design.⁷ It is perhaps a bit extreme to say that this explosion of interest has ushered in a “fluorine renaissance,” but the new appreciation fluorine has recently gained from multiple fields of science is quite notable. Because of this, interest in the properties of organofluorine molecules has experienced phenomenal growth with each passing year.⁸ For fluorine to reach its potential, more information of its properties and how it acts in complex systems is desirable.⁹ From both a medicinal and academic standpoint, an especially intriguing facet is the way that C–F bonds interact with other *extremely proximate functional groups*, especially intramolecularly.¹⁰ With the noted success of fluorination in medicine, this information could help pave the way for designing new fluorinated drugs that interact better with biological systems.¹¹ In the realm of synthetic chemistry, exploitation of fluorine’s unique acceptor properties has imparted stereoselectivity to new reactions.¹² Due to their ubiquity in organic chemistry and the lively debate surrounding the C–F bond’s ability as a hydrogen bond acceptor, interaction with proximate, C–H bonds would be of special interest.^{13,14}

Herein, we document the properties of a series of molecules in which the nature of a C–F---H–C interaction can be modulated by hydrogen bonding that is induced by the

placement of functional groups geminal to the H–C bond. Electronic effects arising from these conditions are documented by X-ray crystallography and IR, ¹H NMR, and ¹⁹F NMR spectroscopy. Depending on the nature of the functional group, both additional *red* and rarer *blue*-shifted hydrogen bonding interactions can be induced relative to a standard molecule. As a starting point for our study, we chose to utilize the easily modifiable cage organofluorine system (**1**, Figure 1). In a recent

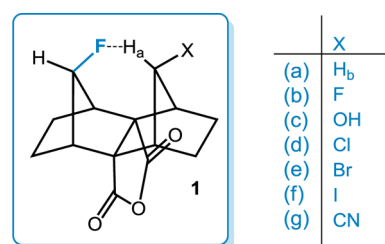


Figure 1. Molecules for the study of through-space (or through-hydrogen bond) fluorine interactions.

article, we employed a variation of this cage framework to generate what we believe to be a transient symmetrical fluoronium ion in situ.¹⁵ The virtue of this system is that it affords a rigid framework in which fluorine is positioned to interact closely with a nearby, conformationally immobile C–H bond. Now imagine the two σ -bonds pointing at each other in close proximity: they almost look like they are about to clash,

Received: August 17, 2013

Published: October 8, 2013

like medieval jousts, in effect, a graphic description of close, nonbonded interactions between spatially proximate bonds such that one or both may experience evident bond compression or distortion. Although the implication is that such interactions are generally strain-inducing, a small bit of hydrogen bonding serves to make the best of a tight situation. We decided to observe if polarizing the “jousting” interaction in the manner of a stronger hydrogen bond would counteract the effect in interesting and heretofore unseen ways and enhance attraction. This is a chance to observe true conformationally locked C–F...H–C hydrogen bonding, which is a generally rare occurrence, and represents a timely problem in fluorine chemistry.¹⁶

The “jousting” effect can be compared to the chemical “iron maiden” interaction, in which a C–H bond experiences compression by its proximity to the π -cloud of an aromatic ring.¹⁷ The “iron maiden” was an apocryphal medieval instrument of torture, consisting of a hinged iron case whose interior is studded with sharp spikes. The σ -bonds in this case serve as the sharp “spikes” of the torture device, the aromatic ring the presumed victim.

Our prototype molecule (X = H_a, **1a**) is an interesting case in itself. From calculation (B3LYP/6-311++G**), an intrabridgehead (H...F) distance of 1.94 Å can be estimated. This is a very close interaction indeed; witness the seminal study of Thalladi et al. on C–H...F interactions in crystalline fluorobenzenes, which indicate typical 2.41–2.78 Å H...F distances.¹⁸ The authors concluded that these constitute weak, but clear, examples of H-bonding. A recent paper by Thakur et al. highlights several other molecules with H...F distances ranging from 2.23 to 2.35 Å.¹⁹ As a point of reference, a basic, prototype C–H...F interaction between two aliphatic centers, methane and fluoromethane, is exceptionally weak as shown by an optimized bond distance in vacuum (2.68 Å at B3LYP/6-311++G**). One can also see that something unusual is going on by comparing the chemical shifts of the *in*-proton that interacts closely with F (H_a) vs the *out* (H_b); in a sense, presenting us with an internal reference. The *out* resonates at δ 1.30, a standard value for methylene groups in hydrocarbons. The *in* resonates at δ 3.16, a downfield shift of almost 2 ppm from analogous systems. While this may appear to be clearly the work of a hydrogen bond, there are some subtleties. There is the extreme forced proximity between the fluorine and hydrogen, which we would expect to result in putative bond compression.²⁰ Hence we have a rarer situation in which a potential H-bonded species exhibits a significant blue-shifted C–H stretch (3108 cm⁻¹). Blue-shifted (or “improper”) X–H...Y hydrogen bonds have become a spirited problem and subject of debate the past decade or so.²¹ Their existence is often attributed to an increase in s-character of the X–H hybrid orbital, as predicted by Bent’s rule,^{22,23} or, as Joseph and Jemmis have alternatively written, to the “electron affinity of X, which causes a net gain of electron density at the X–H bond region in the presence of Y.”²¹ Spin–spin coupling constants are also very illustrative; a primarily through-space (which could also be termed a “through hydrogen bond”²⁴) H–F spin–spin coupling of 12 Hz was observed.²⁵ On the other hand, although electron density (ρ) calculations using the quantum theory of atoms in molecules (AIM) program²⁶ indicate a bond critical point (BCP) between H and F, its magnitude represents a borderline weak/moderate H-bonding interaction (ρ at BCP = 2.4×10^{-2}).^{27–29} In this case, it may be

that we have some interplay of weak hydrogen bonding and nonbonded repulsion (the jousting).

At this point, we sought to make a series of substituted cage molecules (**1b–g**) from previously characterized starting materials as points of comparison (see Figure 2). Molecule

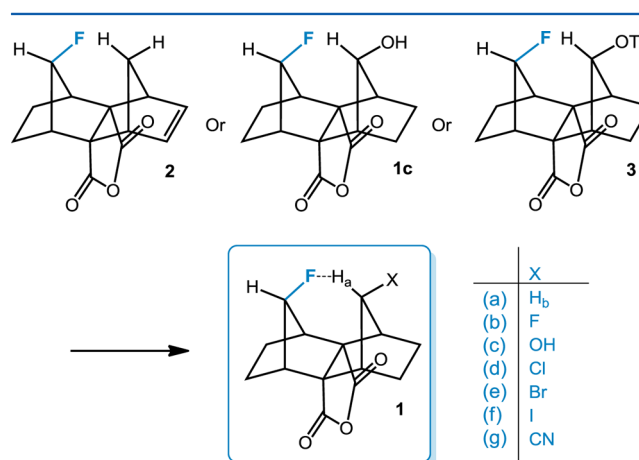


Figure 2. Precursor molecules for the syntheses of the various derivatives of **1** (synthetic procedures are available in the Experimental Section).

1a was synthesized by hydrogenation of **2**,^{15b} alcohol **1c** served as the substrate for the synthesis of **1b** (treatment with DAST), and **1d**, **1e**, **1f**, and **1g** were all made through triflation of **1c** followed by treatment with NaCl, NaBr, NaI, or NaCN in DMF or acetone. The S_N1 reactions of **1d–g** proceeded with no discernible rearrangements to the molecule’s structure, likely due to the effect of the electron-withdrawing capabilities of the anhydride ring.³⁰ We chose substituents that were fairly nonsterically demanding yet homologous, namely halides and the hydroxyl group. As can be seen in Table 1, the magnitude of $J_{\text{H–F}}$ -coupling, which should correlate to the strength of the through-space interaction³¹ (H_a...F), increases in the order H < F ~ OH < Cl < Br < I, paralleling the increase in frequency of the IR stretch of C–H_a (which hybrid DFT calculations show is indeed heavily localized on the C–H_a bond). The largest shift in the IR spectrum occurred for X = I (**1f**), in which the H stretch resonates at 3156 cm⁻¹, representing a 48 cm⁻¹ blue shift from the C–H_a stretch of **1a** (and a ca. 190 cm⁻¹ blue shift from the one carbon bridge of norbornane³²). As it has been observed in other blue-shifted systems, the intensity of the IR stretches is generally low.²³ The large through-space coupling between the bridgeheads ($J_{\text{H–F}}$ = 25.3 Hz) is also maximized for the halides in this molecule.

We obtained a crystal structure of **1f** and compared it to the calculated equilibrium structure at the B3LYP/6-311++G** level (Figure 3). Due to the low scattering power of the H atoms in X-ray diffraction the locations of the H atoms cannot be accurately determined; thus, the C–H bond length had to be constrained to 1.071(10) Å to match the calculated value obtained from DFT calculations. The F...H distances in both structures are close, with 1.837(18) Å for the crystal structure and 1.842 Å for the calculation, reflecting an anticipated downward trend in F...H distances with increasing J values. AIM calculations also show an upward trend of electron density (as well as a positive Laplacian of the electron density) at the bond critical points of the H...F interactions, surpassing the threshold for moderate hydrogen bonding.³³ A natural bond

Table 1. Spectroscopic and Computational Data

X (1)	$J(^1\text{H}_a\text{--}^{19}\text{F})$ (Hz)	$\delta^1\text{H}_a$ NMR	$\rho(10^{-2})^a$	$d(\text{F--H})$ (Å)	%s C–H ^c	ν (C–H stretch, cm^{-1})	$d(\text{C--H})^c$ (Å)	natural charge for H_a^c	natural charge for C^c
H (1a)	12.2	3.16 (1.30 ^b)	2.4	1.906	26.1 (23.9)	3108	1.078 (1.094)	0.24 (0.20)	−0.39 (−0.39)
F (1b)	17.5	6.32	2.6	1.885	27.6 (25.4)	3135	1.077 (1.093)	0.21 (0.17)	0.23 (0.24)
OH (1c)	18.7	5.68	2.6	1.874	26.6 (24.5)	3134	1.078 (1.098)	0.21 (0.16)	0.11 (0.13)
Cl (1d)	24.5	5.68	2.8	1.844	27.6 (25.5)	3146	1.074 (1.089)	0.25 (0.21)	−0.19 (−0.18)
Br (1e)	24.5	5.84	2.9	1.844	28.0 (25.9)	3152	1.073 (1.088)	0.25 (0.21)	−0.25 (−0.24)
I (1f)	25.3	5.85	2.9	1.842	28.4 (26.2)	3156	1.073 (1.088)	0.25 (0.22)	−0.33 (−0.32)
CN (1g)	30.7	4.56	3.0	1.826	24.8 (23.2)	3082	1.081 (1.094)	0.28 (0.244)	−0.35 (−0.35)

^a ρ equals electron density at BCP (bond critical point). Optimizations performed at B3LYP/6-311++G** (B3LYP/DGDZVP on I). ^bOut hydrogen. ^cValues in parentheses are for norbornanes in which X is placed in the 7-position.

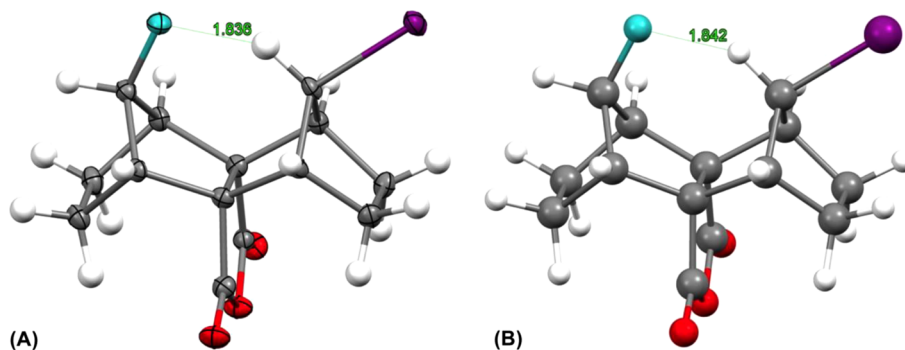


Figure 3. (a) Crystal structure of 1f determined from single-crystal X-ray diffraction. The C–H_a distance was constrained to the value calculated in the DFT equilibrium calculation (1.073 Å). (b) Equilibrium structure calculation of 1f at B3LYP/6-311++G** (B3LYP/DGDZVP on I).

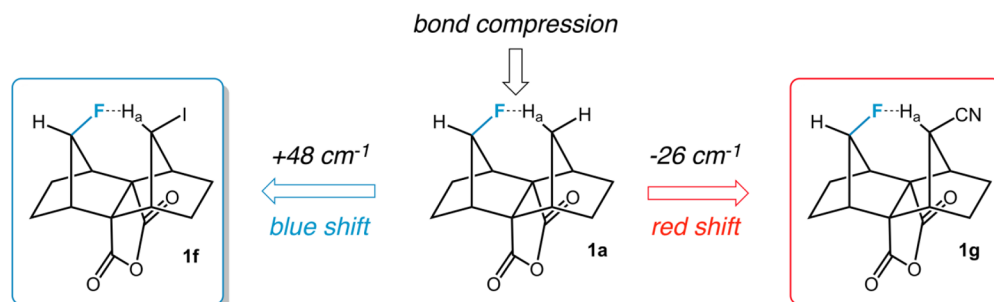


Figure 4. Blue versus red shifts in C–F...H–C interactions.

order analysis also provides some clues; for example, the percent s-character of the carbon-centered hybrid orbital of the C–H bond trends upward in line with the IR stretch, resulting in a stronger C–H bond. Larger halogens, engaging in longer bonds, are thus observed to impart additional s-character to the remaining hybrid orbitals, in concord with Bent's rule, thereby enhancing H-bonding and alleviating bond compression.³⁴ This trend is also present in parallel calculations on 7-substituted norbornanes, which can be seen as non-hydrogen bonded standards (see Table 1). However, one can also see that computed bond lengths are shortened in our study molecules relative to norbornanes, a consequence in part on bond compression; natural atomic charges also show a polarization of H_a relative to the norbornanes as well. Thus, we have several more apparent cases of blue-shifted hydrogen bonds (relative to 1a and the norbornanes), the most dramatic of which is represented by the iodide 1f, in which the shift can be attributed to an increase in the s-character of the C–H hybrid orbital from reference molecule 1a.

After exhausting the halides, we wondered: what would happen if we instead attached a sterically unencumbered

resonance electron-withdrawing substituent to the C–H bond? To achieve the desired effect, we imagined the placement of a cyano group (R = CN) geminal to H_a as ideal. It is often thought of as being a “pseudo-halogen,” and has a comparable steric demand (namely fairly low). Similarly, an AIM calculation indicates significantly enhanced electron density residing between H...F ($\rho = 3.0 \times 10^{-2}$). How should this translate spectroscopically? In fact, a significant red shift relative to the prototype molecule 1a (1g, 3082 cm^{-1}) was observed (but still blue-shifted relative to 7-norbornyl derivatives). H...F coupling is also large, as in 1f (X = I) (30.7 Hz [calcd At B3LYP/6-311++G** using the GIAO method to be 26 Hz]), suggesting a more powerful interaction between H and F. Long-range spin–spin couplings between ¹³C–H_a and ¹⁹F are also very large – whereas for 1a (X = H) the coupling is 38 Hz, for X = I and CN (1f and 1g respectively) it is 50 Hz. The C–H bond stretch is red-shifted relative to the iodide by 74 cm^{-1} , yet AIM predicts comparable ρ values at the bond critical point, correlating with the ¹⁹F...H_a couplings. The s-character of the C–H hybrid has now dropped to 24.8%, revealing a trend in the opposite direction. Here the resonance electron with-

drawing character of the cyano group plays a role through hyperconjugation with the C–H bond.³⁵ In Figure 4, we compare the effects of iodo (**1f**, blue shift) versus cyano (**1g**, red shift) substitution on the C–H_α stretches.

CONCLUSIONS

We have found that a series of cage molecules, with their rigidity, forced proximity of H and F atoms as well as their versatility, provide ideal systems for the investigation of “jousting” interactions. Our results show clear indications of both F...H hydrogen bonding interactions as well as C–H bond compression enforced by the cage framework of the study molecules. There also appears to be a clear correlation between percent s-character in C–H hybrids with the blue-shifted H-bond examples; this trend can be counteracted by the placement of a resonance electron-withdrawing cyano group on the cage system to afford a red-shifted interaction (relative to a standard molecule). Most importantly, in this series of molecules, the size of the through-space H–F spin–spin couplings may be indicative of the strength of the interactions; this conclusion is supported by AIM calculations.

EXPERIMENTAL SECTION

General Methods. Unless otherwise stated, all reactions were carried out under strictly anhydrous, air-free conditions under nitrogen. All solvents and reagents were dried and distilled by standard methods. ¹H and ¹³C spectra were acquired on a 400 MHz NMR in CDCl₃ at 25 °C; ¹⁹F spectra were taken on a 300 MHz NMR in CDCl₃ at 25 °C. The ¹H, ¹³C, and ¹⁹F chemical shifts are given in parts per million (δ) with respect to an internal tetramethylsilane (TMS, δ 0.00 ppm) standard and/or CFCl₃ (δ 0.00 ppm). NMR data are reported in the following format: chemical shifts (multiplicity (s = singlet, d = doublet, t = triplet, q = quartet, m = multiplet), integration, coupling constants (Hz)). IR data were obtained using an FT-IR with a flat CaF₂ cell. HRMS calculations were performed on an ESI-TOF mass spectrometer. All measurements were recorded at 25 °C unless otherwise stated. Melting points are uncorrected. Compounds (**1c**, **2**, and **3**) were prepared according to literature procedures.¹⁵ Spectral data was processed with ACD/NMR Processor Academic Edition.³⁶

Computational Methods. The Gaussian 09 package and Spartan '10 were used for all geometry optimizations.^{37,38} The ¹⁹F calculated chemical shifts were fitted to the empirical equation (at B3LYP/6-311++G**) $\delta_{\text{calc}} = -0.914\delta + 141.83$.³⁹ Geometry optimizations were likewise determined using the B3LYP/6-311++G** level. Atoms in molecules (AIM) calculations were performed using the program AIMAll on structures optimized to B3LYP/6-311++G**.²⁶

Compound Characterization. (*1R,4S,4aR,5S,8R,12S*)-12-Fluoro-octahydro-1,4:5,8-dimethano-4a,8a-(methanooxymethano)naphthalene-9,11-dione (**1a**). Compound **2** (0.097 g, 0.391 mmol) was dissolved in THF (5 mL). The solution was treated with Pd/C catalyst (0.01 g) and hydrogen gas at 2 bar in a Parr apparatus for 12 h. The mixture was then filtered through Celite and concentrated under reduced pressure to yield **1a** as white crystals (0.089 g, 91% yield): mp = 188 °C; ¹H NMR (CDCl₃) δ 4.96 (d, 1H, J = 61.6 Hz), 3.15 (t, 1H, J = 12.3 Hz), 2.62 (m, 2H), 2.60 (s, 2H), 1.80 (d, 2H, J = 9.9 Hz), 1.75 (d, 2H, J = 9.1 Hz), 1.56–1.48 (m, 4H), 1.30 (dd, 1H, J = 11.7, 8.0 Hz); ¹³C NMR (CDCl₃) δ 174.2, 101.4 (d, J = 213.7 Hz), 70.6, 44.3 (d, J = 15.37 Hz), 42.3, 38.7 (d, J = 38.1 Hz), 28.1, 23.5 (d, J = 10.2 Hz); ¹⁹F NMR (CDCl₃) δ –173.04 (dm, 1F, J = 61.9 Hz); IR 3108, 2983, 2966, 2898, 1850, 1774 (cm⁻¹, CaF₂, CH₂Cl₂); HRMS (ESI+) calcd for NaC₁₄H₁₅FO₃ 273.0903, found 273.0907.

(*1R,4S,4aR,5R,8S,12S,13S*)-12,13-Difluoro-octahydro-1,4:5,8-dimethano-4a,8a-(methanooxymethano)naphthalene-9,11-dione (**1b**). A solution of **1c** (21 mg, 0.08 mmol) in 5 mL of dichloromethane (DCM) was cooled to –78 °C with stirring. To the solution diethylaminosulfur trifluoride (DAST) (0.021 mL, 0.16 mmol) was added dropwise, and the solution was stirred for 1 h at

–78 °C. The reaction was then quenched with saturated aqueous sodium bicarbonate (4 mL). The organic layer was separated, dried with magnesium sulfate, and filtered through Celite, and the solvent was removed under reduced pressure. The crude product was purified by silica gel flash column chromatography with a 10% ethyl acetate and hexanes solution to yield **1b** as white crystals (5 mg, 23% yield): mp = 153 °C; ¹H NMR (CDCl₃) δ 6.32 (dd, 1H, J = 56.1, 18.0 Hz), 4.99 (d, 1H, J = 61.6 Hz), 2.68 (q, 2H, J = 4.8, 2.3 Hz), 2.64 (s, 2H), 2.12 (d, 2H, J = 11.9 Hz), 1.82 (d, 2H, J = 10.4 Hz), 1.56 (d, 2H, J = 4.5 Hz), 1.51 (t, 2H, J = 9.1 Hz); ¹³C NMR (CDCl₃) δ 173.0 (d, J = 1.5 Hz), 101.22 (d, J = 213.7 Hz), 96.1 (q, J = 242.2, 53.4 Hz), 66.5 (d, J = 8 Hz), 44.3 (d, J = 14.6 Hz), 44.0 (d, J = 16.1), 24.3 (d, J = 5.9 Hz), 23.3 (d, J = 9.5 Hz); ¹⁹F NMR (CDCl₃) δ –178.90 (dm, 1F, J = 60.8 Hz), –198.51 (dd, 1F, J = 55.7, 19.6 Hz); IR 3135, 2962, 2925, 2858, 1861, 1783, 1725 (cm⁻¹, CaF₂, CH₂Cl₂); HRMS (ESI+) calcd for NaC₁₄H₁₄F₂O₃ 291.0809, found 291.0802.

(*1R,4S,5R,8S,8aR,12S,13S*)-12-Fluoro-13-hydroxyoctahydro-1,4:5,8-dimethano-4a,8a-(methanooxymethano)naphthalene-9,11-dione (**1c**). White solid, 0.23 g (87% yield); synthesized by following the synthetic route reported in literature.¹⁵ Spectral and analytical data were in agreement with previous reports.

(*1R,4S,4aS,5R,8S,12S,13S*)-12-Chloro-13-fluoro-octahydro-1,4:5,8-dimethano-4a,8a-(methanooxymethano)naphthalene-9,11-dione (**1d**). To a solution of compound **3** (68 mg, 0.171 mmol) in 5 mL of dry N,N-dimethylformamide (DMF) was added sodium chloride (40 mg, 0.684 mmol). The solution was heated to 70 °C with stirring in a sealed tube and was allowed to react for 20 h. The solution was then poured into ice-cold water (20 mL) and extracted with EtOAc (3 × 15 mL). The organic layers were combined, dried with magnesium sulfate, filtered through Celite, and concentrated under reduced pressure. The crude product was then purified by silica gel flash column chromatography with a 20% ethyl acetate and hexanes solution to yield **1d** as white crystals (17.3 mg, 36% yield): mp = 135 °C; ¹H NMR (CDCl₃) δ 5.77 (d, 1H, J = 24.5 Hz), 5.02 (d, 1H, J = 62.0 Hz), 2.67 (q, 4H, J = 4.3, 1.9 Hz), 2.29 (d, 2H, J = 9.6 Hz), 1.84 (d, 2H, J = 10.7 Hz), 1.62–1.45 (m, 4H); ¹³C NMR (CDCl₃) δ 172.8, 101.5 (d, J = 213.7 Hz), 68.4, 62.9 (d, J = 52.7 Hz), 47.0, 44.3 (d, J = 14.6 Hz), 24.9, 23.4 (d, J = 9.5 Hz); ¹⁹F NMR (CDCl₃) δ –173.9 (ddt, 1F, J = 61.9, 24.7, 9.3 Hz); IR 3146.4, 3061.4, 2988.1, 2903.1, 1862.7, 1789.4 (cm⁻¹, CaF₂, CH₂Cl₂); HRMS (ESI+) calcd for NaC₁₄H₁₄ClFO₃ 307.0513, found 307.0510.

(*1R,4S,4aS,5R,8S,12S,13S*)-12-Bromo-13-fluoro-octahydro-1,4:5,8-dimethano-4a,8a-(methanooxymethano)naphthalene-9,11-dione (**1e**). To a solution of compound **3** (42 mg, 0.106 mmol) in 5 mL of dry acetone was added potassium bromide (51 mg, 0.424 mmol). The solution was heated to 70 °C with stirring in a sealed tube and was allowed to react for 48 h. The solvent was removed under reduced pressure, and the resulting residue was dissolved in DCM (10 mL) and washed with water (2 × 10 mL). The organic layer was then dried with magnesium sulfate, filtered through Celite and concentrated under reduced pressure. The crude product was then purified by flash column chromatography on florisil 60–100 mesh with a 10% ethyl acetate and hexanes solution to yield **1e** as white crystals (9.1 mg, 26% yield); mp = 157 °C; ¹H NMR (CDCl₃) δ 5.84 (d, 1H, J = 24.8 Hz), 5.03 (d, 1H, J = 62.4 Hz), 2.72 (q, 2H, J = 4.6, 1.8), 2.68 (s, 2H), 2.33 (d, 2H, J = 9.6), 1.84 (d, 2H, J = 9.3), 1.61 (d, 2H, J = 8.8 Hz), 1.51 (t, 2H, J = 9.1 Hz); ¹³C NMR (CDCl₃) δ 172.6, 101.6 (d, J = 214.4 Hz), 68.2, 54.0 (d, J = 51.96), 47.3, 44.2 (d, J = 14.6 Hz), 25.8, 23.4 (d, J = 9.5 Hz); ¹⁹F NMR (CDCl₃) δ –173.71 (ddt, 1F, J = 61.9, 24.8, 8.3 Hz); IR 3152, 2962, 2926, 2853, 1865, 1783 (cm⁻¹, CaF₂, CH₂Cl₂); HRMS (ESI+) calcd for NaC₁₄H₁₄BrFO₃ 351.0008, found 351.0015.

(*1R,4S,5R,8S,8aS,12S,13S*)-12-Fluoro-13-iodooctahydro-1,4:5,8-dimethano-4a,8a-(methanooxymethano)naphthalene-9,11-dione (**1f**). To a solution of compound **3** (110 mg, 0.276 mmol) in 5 mL of dry acetone was added sodium iodide (165 mg, 1.1 mmol). The solution was heated to 70 °C with stirring in a sealed tube and was allowed to react for 20 h. The solvent was removed under reduced pressure, and the resulting residue was dissolved in DCM (10 mL) and washed with water (2 × 10 mL). The organic layer was then dried with magnesium sulfate, filtered through Celite and concentrated under reduced pressure. The crude product was then purified by silica gel

flash column chromatography with a 20% ethyl acetate and hexanes solution to yield **1f** as white crystals that gradually turned brown when exposed to light (33.8 mg, 33% yield): mp = 167 °C; ¹H NMR (CDCl₃) δ 5.86 (d, 1H, J = 25.3 Hz), 5.03 (d, 1H, J = 62.9 Hz), 2.70 (s, 2H), 2.67 (s, 2H), 2.33 (d, 2H, J = 10.6 Hz), 1.83 (d, 2H, J = 10.1 Hz), 1.66 (d, 2H, J = 10.1), 1.52 (t, 2H, J = 8.6 Hz); ¹³C NMR (CDCl₃) δ 172.4, 101.6 (d, J = 214.4 Hz), 67.5, 48.3, 44.3 (d, J = 14.6 Hz), 30.1 (d, J = 49.8 Hz), 27.4 (d, J = 2.2 Hz), 23.44 (d, J = 11.0 Hz); ¹⁹F NMR (CDCl₃) δ -173.16 (ddt, 1F, J = 61.9, 25.8, 8.3 Hz); IR 3156, 2961, 2908, 1867, 1772 (cm⁻¹, CaF₂, CH₂Cl₂); HRMS (ESI+) calcd for NaC₁₄H₁₄IFO₃ 398.9869, found 398.9873.

X-ray data for 1f: Fw = 376.15, irregular colorless shaped crystals, 0.28 × 0.16 × 0.08 mm³, monoclinic, C2/c (no. 15), a = 21.9855(4) Å, b = 8.06787(16) Å, c = 13.8359(3) Å, β = 91.2493(18)°, V = 2453.58(8) Å³, Z = 8, D_x = 2.037 g cm⁻³, μ = 20.665 mm⁻¹, T_{min} – T_{max}: 0.061–0.335. 8673 reflections were measured up to a resolution of (sin θ/λ)_{max} = 0.62 Å⁻¹. 2407 reflections were unique (R_{int} = 0.0207), of which 2336 were observed [I > 2σ(I)]. 177 Parameters were refined. R1/wR2 [I > 2σ(I)]: 0.0181/0.0465. R1/wR2 [all refl.]: 0.0187/0.0469. S = 1.051. Residual electron density found between -0.51 and 0.76 e Å⁻³.

(1R,4S,4aR,5S,8R,12S,13S)-13-Fluoro-9,11-dioxooctahydro-1,4,5,8-dimethano-4a,8a-(methanooxymethano)naphthalene-12-carbonitrile (**1g**). To a solution of compound **3** (22 mg, 0.056 mmol) in 5 mL of dry N,N-dimethylformamide (DMF) was added sodium cyanide (11 mg, 0.22 mmol). The solution was heated to 80 °C with stirring in a sealed tube and was allowed to react for 20 h. The solution was then poured into ice-cold water (20 mL) and extracted with EtOAc (3 × 15 mL). The organic layers were combined, dried with magnesium sulfate, filtered through Celite, and concentrated under reduced pressure. The crude product was then purified by silica gel flash column chromatography with a 20% ethyl acetate and hexanes solution to yield **1g** as white crystals (12.2 mg, 79% yield): mp = 174 °C; ¹H NMR (CDCl₃) δ 5.04 (d, 1H, J = 62.7 Hz), 4.56 (d, 1H, J = 30.8 Hz), 2.91 (q, 2H, J = 4.6, 1.8 Hz), 2.7 (s, 2H), 2.28 (d, 2H, J = 9.9 Hz), 1.87 (d, 2H, J = 9.3 Hz), 1.71 (d, 2H, J = 8.6 Hz), 1.56–1.49 (m, 2H); ¹³C NMR (CDCl₃) δ 171.92, 118.7, 101.6 (d, J = 213.0 Hz), 69.6, 45.2, 44.3 (d, J = 13.9 Hz), 38.0 (d, J = 49.8 Hz), 26.0, 23.3 (d, J = 9.5 Hz); ¹⁹F NMR (CDCl₃) δ -170.23 (ddt, 1F, J = 62.9, 30.9, 8.3 Hz); IR 3082, 2962, 2926, 2868, 2854, 1859, 1783 (cm⁻¹, CaF₂, CH₂Cl₂); HRMS (ESI+) calcd for NaC₁₃H₁₄FNO₃ 298.0855, found 298.0859.

(1R,4S,4aR,5R,8S,13S)-13-Fluoro-1,2,3,4,5,8-hexahydro-1,4,5,8-dimethano-4a,8a-(methanooxymethano)naphthalene-9,11-dione (**2**). White solid, 0.43 g (33% yield); synthesized by following the synthetic route reported in literature.¹⁵ Spectral and analytical data were in agreement with previous reports.

(1R,4S,4aR,5R,8S,12S,13S)-13-Fluoro-9,11-dioxooctahydro-1,4,5,8-dimethano-4a,8a-(methanooxymethano)naphthalen-12-yl Trifluoromethanesulfonate (**3**). White solid, 0.31 g (94% yield); synthesized from **1c**. Spectral and analytical data were in agreement with previous reports.¹⁵

■ ASSOCIATED CONTENT

📄 Supporting Information

NMR spectra, X-ray parameters, and computational data. This material is available free of charge via the Internet at <http://pubs.acs.org>.

■ AUTHOR INFORMATION

✉ Corresponding Author

*E-mail: lectka@jhu.edu.

Notes

The authors declare no competing financial interest.

■ ACKNOWLEDGMENTS

T.L. thanks the NSF (CHE 1152996) for a grant. M.D.S. thanks Johns Hopkins for a Gary H. Posner fellowship. We

would like to thank Prof. Gerald J. Meyer for the use of his FT-IR.

■ REFERENCES

- (1) Filler, R.; Saha, R. *Future Med. Chem* **2009**, *5*, 777–791.
- (2) Maienfisch, P.; Hall, R. G. *Chimia* **2004**, *58*, 93–99.
- (3) Kitazume, T. *J. Fluorine Chem.* **2000**, *105*, 265–278.
- (4) Shimizu, M.; Hiyama, T. *Angew. Chem., Int. Ed.* **2005**, *44*, 214–231.
- (5) Bégué, J.; Bonnet-Delpon, D. *J. Fluorine Chem.* **2006**, *127*, 992–1012.
- (6) Isanbor, C.; O'Hagan, D. *J. Fluorine Chem.* **2006**, *127*, 303–319.
- (7) Ojima, I. *J. Org. Chem.* **2013**, *78*, 6358–6383.
- (8) Müller, K.; Faeh, C.; Diederich, F. *Science* **2007**, *317*, 1881–1886.
- (9) Kirk, K. L. *J. Fluorine Chem.* **2006**, *127*, 1013–1029.
- (10) Nishide, K.; Hagimoto, Y.; Hasegawa, H.; Shiro, M.; Node, M. *Chem. Commun.* **2001**, 2394–2395.
- (11) Wilcken, R.; Zimmermann, M. O.; Lange, A.; Joerger, A. C.; Boeckler, F. M. *J. Med. Chem.* **2013**, *56*, 1363–1388.
- (12) (a) Gold, B.; Shevchenko, N. E.; Bonus, N.; Dudley, G. B.; Alabugin, I. V. *J. Org. Chem.* **2012**, *77*, 75–89. (b) Gold, B.; Dudley, G. B.; Alabugin, I. V. *J. Am. Chem. Soc.* **2013**, *135*, 1558–1569.
- (13) Schneider, H. *Chem. Sci.* **2012**, *3*, 1381–1394.
- (14) Dunitz, J. D.; Taylor, R. *Chem.—Eur. J.* **1997**, *3*, 89–98.
- (15) (a) Struble, M. D.; Scerba, M. T.; Siegler, M. A.; Lectka, T. *Science* **2013**, *340*, 57–60. (b) The synthesis and very preliminary study of a prototype of this cage system was also reported: Scerba, M. T.; Bloom, S.; Haselton, N.; Siegler, M.; Jaffe, J.; Lectka, T. *J. Org. Chem.* **2012**, *77*, 1605–1609.
- (16) (a) Howard, J. A. K.; Hoy, V. J.; O'Hagan, D.; Smith, G. T. *Tetrahedron* **1996**, *52*, 12613–12622. (b) Chan, M. C. W.; Kui, S. C. F.; Cole, J. M.; McIntyre, G. J.; Matsui, S.; Zhu, N.; Tam, K.-H. *Chem.—Eur. J.* **2006**, *12*, 2607–2619.
- (17) Pascal, R. A., Jr. *Eur. J. Org. Chem.* **2004**, 3763–3771.
- (18) Thalladi, V. R.; Weiss, H.; Bläser, D.; Boese, R.; Nangia, A.; Desiraju, G. R. *J. Am. Chem. Soc.* **1998**, *120*, 8702–8710.
- (19) Thakur, T. S.; Kirchner, M. T.; Bläser, D.; Boese, R.; Desiraju, G. R. *CrystEngComm* **2010**, *12*, 2079–2085.
- (20) For more information on the effects of bond compression on NMR, see: (a) Lawson, M. N.; Blanda, M. T.; Staggs, S. J.; Sederholm, L. N.; Easter, D. C. *J. Phys. Org. Chem.* **2009**, *22*, 1212–1224. (b) Kleinpeter, E.; Szatmári, I.; Lázár, L.; Koch, A.; Heydenreich, M.; Fülöp, F. *Tetrahedron* **2009**, *65*, 8021–8027.
- (21) Jemmis and Joseph have organized a nice discussion of the theory of blue-shifted or “improper” H-bonds: Joseph, J.; Jemmis, E. D. *J. Am. Chem. Soc.* **2007**, *129*, 4620–4632.
- (22) (a) Alabugin, I. V.; Manoharan, M.; Peabody, S.; Weinhold, F. *J. Am. Chem. Soc.* **2003**, *125*, 5973–5987. (b) Alabugin, I. V.; Manoharan, M. *J. Comput. Chem.* **2006**, *28*, 373–390.
- (23) Bent, H. A. *Chem. Rev.* **1968**, *68*, 587–648.
- (24) Bagno et al. have pointed out the equivalence of through-space and through-H-bond couplings; see: Bagno, A.; Saielli, G.; Scorrano, G. *Chem.—Eur. J.* **2002**, *8*, 2047–2056.
- (25) For pioneering examples of through-space H–F couplings, see: (a) Adcock, W.; Rizvi, S. Q. *Aust. J. Chem.* **1973**, *26*, 2659–2663. (b) Yamamoto, G.; Oki, M. *J. Org. Chem.* **1984**, *49*, 1913–1917.
- (26) AIMAll (Version 13.05.06): Keith, T. A. TK Gristmill Software, Overland Park KS, 2013 (aim.tkgristmill.com).
- (27) Bader, R. F. W. *Acc. Chem. Res.* **1985**, *18*, 9–15.
- (28) The calculated laplacian of the charge density at the bond critical point > 0 for **1a–g**, consistent with a “charge shift” or weak-moderate hydrogen bond; see: Grabowski, S. J. *J. Phys. Chem. A* **2011**, *115*, 12789–12799.
- (29) Parthasarathi, R.; Subramanian, V.; Sathyamurthy, N. *J. Phys. Chem. A* **2006**, *110*, 3349–3351.
- (30) For a discussion of similar reactions involving solvolyses of **3** see ref 13.
- (31) Chaudhari, S. R.; Mogurampelly, S.; Suryaprakash, N. *J. Phys. Chem. B* **2013**, *117*, 1123–1129.

- (32) NIST Mass Spec Data Center, Stein, S. E., Director.
- (33) Koch, U.; Popelier, P. L. A. *J. Phys. Chem.* **1995**, *99*, 9747–9754.
- (34) Grabowski, S. J. *J. Phys. Chem. A* **2011**, *115*, 12340–12347.
- (35) Salzner, U.; Schleyer, P. v. R. *Chem. Phys. Lett.* **1992**, *190*, 401–406.
- (36) ACD/ChemSketch Freeware, Version 12.01, Advanced Chemistry Development, Inc., Toronto, ON, www.acdlabs.com, 2012.
- (37) Gaussian 09, Revision A.1: Frisch, M. J. et al. Gaussian, Inc., Wallingford CT, 2009.
- (38) Spartan '10 Program, Wavefunction Inc., Irvine, CA.
- (39) Merrick, J. P.; Moran, D.; Radom, L. *J. Phys. Chem. A* **2007**, *111*, 11683–11700.